AIMS Mathematics, 10(8): 18660–18679.
DOI: 10.3934/math.2025834
Received: 28 June 2025
Revised: 07 August 2025
Accepted: 11 August 2025
Published: 18 August 2025

https://www.aimspress.com/journal/Math

Research article

Modeling Monkeypox dynamics with human–rodent interactions and waning vaccination

Turki D. Alharbi[1] and Md Rifat Hasan[2,*]

[1] Department of Mathematics, Al-Leith University College, Umm Al-Qura University, Mecca 24382, Saudi Arabia
[2] Department of Applied Mathematics, Faculty of Science, Noakhali Science and Technology University, Noakhali 3814, Bangladesh

* **Correspondence:** Email: rifatmathdu@gmail.com; Tel: +8801719422462.

Abstract: The global outbreak of the monkeypox virus (Mpox) in 2022–2023, which affected over 100 countries, has underscored the urgent need for robust public health interventions and predictive modeling tools. In this study, we develop a novel mathematical model that captures the transmission dynamics of Mpox between human and rodent populations, incorporating both direct and environmental transmission pathways as well as the effects of vaccination. We prove the model's positivity and boundedness to ensure epidemiological feasibility. Using the next-generation matrix method, we derive the basic reproduction number and assess the local and global stability of both disease-free and endemic equilibria through Lyapunov-based techniques. Sensitivity analysis identifies critical parameters influencing Mpox spread and informs targeted intervention strategies. Numerical simulations illustrate how varying key parameters such as vaccination rates, recovery rates, and transmission pathways affect disease progression. The results emphasize that increasing vaccination coverage and enhancing recovery rates can significantly reduce disease burden. This model provides a comprehensive framework to support evidence-based public health decision-making for controlling future Mpox outbreaks.

Keywords: Monkeypox virus (Mpox); vaccination; Lyapunov; sensitivity; global stability
Mathematics Subject Classification: 34D08, 34D20, 34D23, 92D30, 93D05, 97M10, 97M60

1. Introduction

In 1958, a smallpox-like outbreak transpired among Singaporean monkeys in Copenhagen, followed by analogous occurrences in the USA [1]. The virus that causes human monkeypox is genetically related to the smallpox virus, both of which are classified in the Poxviridae family and the Orthopoxvirus genus [2]. The inaugural human case of monkeypox was documented in the Democratic Republic of the Congo in 1970. Initiatives to eliminate smallpox resulted in the cessation of vaccinations by 1980, diminishing immunity to other viruses within the same family. Over time, monkeypox cases proliferated internationally, culminating in a global epidemic declared by the World Health Organization in July 2022 [3].

The Mpox virus exhibits multiple transmission pathways, encompassing animal-to-human, human-to-human, and environmental routes [4,5]. Transmission from animals to humans takes place when individuals have direct physical interactions with infected wildlife, including species like rodents and primates. Transmission between individuals primarily occurs through close interactions with infected individuals, which include face-to-face encounters, skin contact, and oral exchanges [6]. This outbreak exhibits a distinctive epidemiological characteristic, marked by a predominant sexual transmission of the virus, especially among men. The virus can persist on the surfaces of objects that patients have touched, and environmental transmission may take place when individuals or animals encounter these items [7]. The risk of infection can be heightened through environmental transmission, particularly when individuals with skin lesions encounter organs or mucous membranes without proper hand hygiene [8].

The Mpox virus, an Orthopoxvirus, is classified within the genus Orthopoxvirus of the Poxviridae family, which includes the smallpox virus. It induces less severe symptoms than smallpox and has variability in intensity among individuals [9]. The incubation period for Mpox generally ranges from 7 to 14 days, though it may extend to 21 days [10]. Prodromal symptoms, including fever, chills, headache, fatigue, lethargy, and lymphadenopathy, typically manifest following the incubation period (Figure 1). The characteristic rash, resembling a blister or ulcer, persists for 2 to 4 weeks [11]. Mpox is often self-limiting; however, vulnerable populations, including newborns, children, pregnant women, and individuals with preexisting immune deficits, may encounter more severe symptoms or complications. The mortality rate for Mpox ranges from 0.1% to 10%, predominantly affecting young, afflicted persons [12].

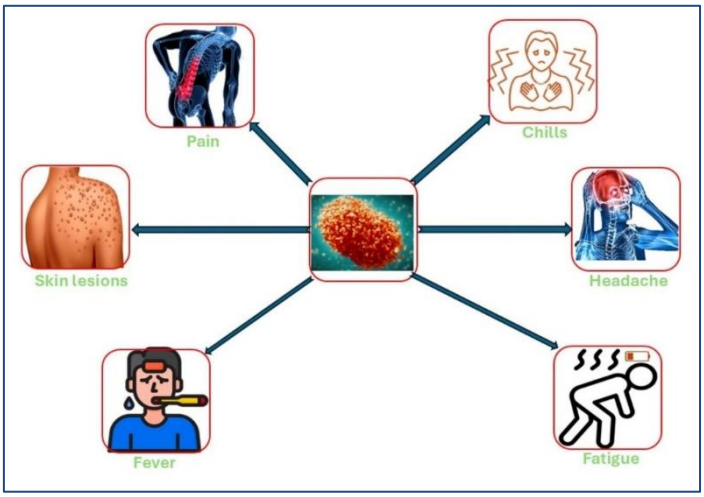

Figure 1. Monkeypox virus clinical characteristics.

Mathematical models can efficiently resolve issues in physical, telecommunications, and technological fields. Furthermore, recent publications illustrate several practical applications of mathematical models [13,14]. A multitude of mathematical models illustrating the transmission and evolution of diseases have been constructed based on published research [15]. Mathematical modeling has been employed to examine the Mpox virus transmission between animals and people as well as among humans. A study investigates the Mpox virus and its two transmission modes: human-to-human and rodent-to-human, without utilizing actual case data. Abidemi et al. [16] presented a mathematical model of Mpox dynamics, incorporating the backward bifurcation characteristic of isolation and quarantine compartments. Kumar et al. [17] presented a mathematical model of Mpox that utilizes both integer and fractional derivatives to simulate the transmission dynamics within the United States. Researchers in [18] analyzed the trends of the Mpox outbreak in the USA using empirical data, discovering a backward bifurcation that renders the model not globally stable in the disease-free scenario. Scholars in [19] employed a continuous model to investigate Mpox transmission, focusing on control interventions, nonlinear trends, bifurcation analysis, and strategies involving treatment, quarantine, vaccination, and awareness initiatives. Awoke et al. [20] established a deterministic conceptual framework to evaluate the Mpox disease cost-effectiveness management techniques, accounting for both direct and indirect transmission impacts on environmental factors. An analytical framework was studied in [21] to predict the effects of ambient viral concentration on disease dynamics and control, with a focus on epidemiological issues and the formulation of control measures. Bentaleb et al. [22] formulated and examined a dual-strain Mpox SEIR model to assess local and global stability, pinpointing the critical thresholds that influence the eradication or endemicity of a clade. Guo and Li [23] developed a compartmental model to analyze the competitive transmission dynamics of the Omicron and Delta COVID-19 strains in the U.S., highlighting strain-specific reproduction numbers and identifying optimal control strategies through cost-effectiveness analysis. An epidemic model for the Delta strain of COVID-19 incorporating imperfect vaccination was developed by Li and Guo [24], and optimal, cost-effective control strategies were identified through parameter estimation and sensitivity analysis using real data from Jiangsu Province, China. Guo and Li [25] proposed a fractional-order model for online game addiction based on real-world data, demonstrating the effectiveness of optimal control strategies using advanced numerical methods and parameter estimation techniques. A novel fractal-fractional operator in the Atangana-Baleanu sense was employed by Manivel et al. [26] to analyze the dynamics of monkeypox and HIV interactions. Omame and colleagues [27] analyzed mathematical mechanisms of Mpox to investigate the potential influence of HIV as well as Mpox within the MSM community. Bragazzi, along with colleagues [28], used a significant compartmental model to examine mpox transmission in Canada, distinguishing between high-risk as well as low-risk populations, and found that adaptive behavioral changes can effectively reduce the ongoing Mpox pandemic among the high-risk population. Liu et al. [29] conducted a fractional-order epidemiological model incorporating imperfect vaccination to analyze monkeypox dynamics, demonstrating the effects of fractional derivatives and key parameters on disease control using U.S. case data. Bansal et al. [30] analyzed Mpox epidemic dynamics, considering vaccination effectiveness, using the Caputo Atangana-Baleanu derivative for theoretical and graphic analysis. The authors of [31] used a deterministic mathematical model inside a constant proportional-Caputo derivative framework to evaluate Mpox and considered human-rodent interactions using actual vaccination settings. Rashid et al. [32] conducted a dynamic analysis and optimum management of a hybrid fractional model for Mpox illness, considering external variables. Ochieng [33] investigated the spread dynamics of Mpox and carried out a cost-effectiveness analysis to determine the most economical Mpox control approach, focusing on an actual scenario in Africa. Shyamsunder & Meena [34] studied the Mpox transmission

outbreak, aiming to enhance mathematical modeling of disease transmission using advanced numerical techniques for effective disease control and mitigation strategies. Idisi et al. [35] constructed a strain-specific epidemiological model to evaluate Mpox transmission dynamics, demonstrating statistical models and epidemic patterns across multiple nations. Rabiu et al. [36] modeled the sexual transmission dynamics of Mpox in the U.S., identifying MSM transmission as the primary driver and highlighting condom use as a critical control measure. Kuga and Tanimoto [37] created an analytical framework integrating evolutionary game theory with the SIR model to assess imperfect vaccination and defense against contagion, finding partial vaccination to be marginally more effective in disease suppression. Tanimoto [38] provided a comprehensive sociophysics-based framework integrating evolutionary game theory and epidemiological modeling to analyze human behavioral responses, such as vaccination and protective measures, during infectious disease outbreaks.

In response to the escalating threat, numerous mathematical models have been developed to understand the transmission dynamics of Mpox. These models have examined various facets, including interpersonal interactions, fractional derivatives for intricate dynamics, and bifurcation analysis. Nonetheless, numerous limitations persist in the current body of research. Many previous investigations employ fragmented modeling approaches that either neglect the significance of rodent reservoirs or address rodent-to-human transmission in an overly simplified manner. This compromises the ability to understand the zoonotic characteristics of Mpox. Additionally, whereas human vaccination is an essential control tool, few models effectively integrate vaccination dynamics into multispecies frameworks. Furthermore, the majority of models prioritize local stability while failing to define global stability conditions, hence constraining their predictive efficacy in practical scenarios. A significant gap exists in employing sensitivity analysis to guide practical control methods, as numerous studies conclude with the identification of sensitive factors without converting them into public health recommendations. Ultimately, dynamic simulations of temporal parameter alterations, especially concerning interactions between rodent and human populations, are infrequently performed, leading to a constrained comprehension of the dynamic effects of interventions on disease progression. To rectify these deficiencies, this study presents several key innovations that extend beyond existing modeling efforts. First, we develop a dual-species transmission framework that explicitly integrates both human and rodent populations, along with the waning effect of vaccination, a critical yet often overlooked aspect of long-term outbreak dynamics. Second, while numerous recent studies have utilized fractional-derivative frameworks or focused solely on human-to-human transmission, our model advances the field by capturing the complete zoonotic transmission cycle and vaccination attrition within a classical deterministic framework. This approach offers both epidemiological realism and mathematical tractability. Finally, the principal mathematical contribution of this work lies in establishing global asymptotic stability using a Lyapunov function-based analysis, which strengthens the predictive reliability of the model and provides theoretical guarantees often lacking in local or purely numerical studies.

The subsequent sections of this work are organized as follows: Section 2 delineates the development of our mathematical model for Monkeypox virus transmission, including both human and rodent populations, as well as a biological rationale for the compartments and corresponding parameters. Section 3 focuses on examining the positivity and boundedness of the model solutions to guarantee epidemiological viability. This part also determines the disease-free and endemic equilibrium points and calculates the fundamental reproduction number R_0 using the next-generation matrix approach. In Section 4, we examine the stability characteristics of the model by evaluating local stability via the eigenvalues of the Jacobian matrix and global stability through Lyapunov function methodologies and relevant theorems. Section 5 addresses sensitivity analysis, evaluating the impact

of specific model parameters on R_0 and finding essential criteria for effective disease control measures. Section 6 delineates the numerical method utilized to resolve the system of differential equations and showcases the resultant simulation outcomes, demonstrating the temporal dynamics of the model across diverse circumstances. Section 7 ultimately finishes the work by summarizing the principal findings and contributions, while delineating avenues for future research, such as model calibration with empirical data, integration of spatial dynamics, and investigation of behavioral reactions in transmission.

2. Formulation of the Monkeypox virus model

Grasping the dissemination patterns of infectious diseases is a crucial investigative step in averting their emergence. This step entails the mathematical modeling of disease dynamics through the application of systems of (ordinary or partial) differential equations. When the transmission dynamics between the interacting species are adequately accounted for, standard existing methods can be utilized to provide insightful mathematical analysis that yields significant biological implications. In developing a conceptual framework to describe Monkeypox virus transmission, it is crucial to consider both human and rodent populations as the primary interacting species, along with the environmental viral load. In this context, our proposed model categorizes the interacting species into the following compartments: susceptible humans S_h, vaccinated humans V_h, exposed humans E_h, infected humans I_h, and recovered humans R_h, while the rodent population is divided into susceptible rodents S_a and infected rodents I_a.

The mathematical framework we introduce is consistent with our assumptions and the descriptions given, as shown in the model flow diagram illustrated in Figure 2, and the biological description of the parameters is itemized in Table 1.

Human population (h)

$$\begin{aligned}
\frac{dS_h}{dt} &= \Lambda_h - \beta_1 S_h I_a - \beta_2 S_h I_h - \alpha_h S_h - \mu_h S_h + \eta V_h,\\
\frac{dV_h}{dt} &= \alpha_h S_h - \eta V_h - \mu_h V_h,\\
\frac{dE_h}{dt} &= \beta_2 S_h I_h + \beta_1 S_h I_a - \alpha_1 E_h - \mu_h E_h,\\
\frac{dI_h}{dt} &= \alpha_1 E_h - \alpha_2 I_h - \delta_h I_h - \mu_h I_h,\\
\frac{dR_h}{dt} &= \alpha_2 I_h - \mu_h R_h.
\end{aligned} \tag{2.1}$$

Rodent population (a)

$$\begin{aligned}
\frac{dS_a}{dt} &= \Lambda_a - \beta_3 S_a I_a - \mu_a S_a,\\
\frac{dI_a}{dt} &= \beta_3 S_a I_a - \mu_a I_a .
\end{aligned}$$

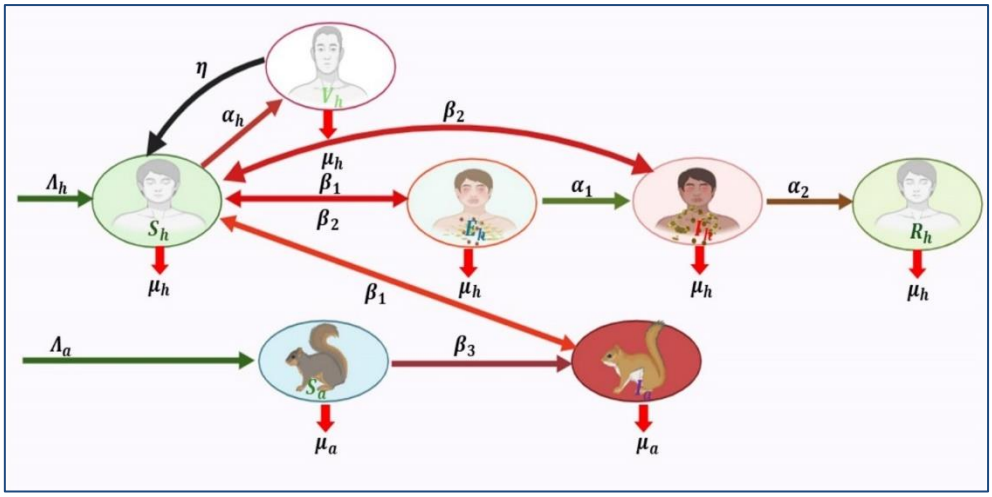

Figure 2. Flow diagram illustration of Monkeypox.

Table 1. Biological descriptions of the Monkeypox model's parameters.

Parameter	Biological Descriptions
Λ_h	Recruitment rates of human population
β_1	Rate of infectious from rodent to human
α_h	Vaccination rate of humans from susceptible class
β_2	Rate of infectious from human to human
μ_h	Natural death rate of human
η	Rate loss of Vaccination effectiveness
α_1	Rate of exposed to infected humans
δ_h	Disease death rate of infected humans
α_2	Recovery rate of infected human
Λ_a	Recruitment rates of rodent
β_3	Infection rate from infected rodent to susceptible rodent
μ_a	Natural death rate of rodent

3. Monkeypox model analyses

3.1. Positivity of the solution

Theorem 3.1. The feasible region

$$\tau = \left\{S_h(0), V_h(0), E_h(0), I_h(0), R_h(0), S_a(0), I_a(0) \epsilon \mathbb{R}_7^+ : N_h(t) \leq \frac{\Lambda_h}{\mu_h}, N_a(t) \leq \frac{\Lambda_a}{\mu_a}\right\}$$

is positively invariant for system (2.1) with initial condition $\mathbb{R}_7^+$.

Proof. System (2.1) can be written as

$$\frac{dY}{dt} = K(Y) + Z. \tag{3.1}$$

$$Y = (S_h, V_h, E_h, I_h, R_h, S_a, I_a)^T,$$

$$K = \begin{pmatrix} -k_1 & \eta & 0 & 0 & 0 & 0 & 0 \\ \alpha_h & -k_2 & 0 & 0 & 0 & 0 & 0 \\ k_3 & 0 & -k_4 & 0 & 0 & 0 & 0 \\ 0 & 0 & \alpha_1 & -k_5 & 0 & 0 & 0 \\ 0 & 0 & 0 & \alpha_2 & -\mu_h & 0 & 0 \\ 0 & 0 & 0 & 0 & 0 & -k_6 & 0 \\ 0 & 0 & 0 & 0 & 0 & k_7 & -\mu_a \end{pmatrix},$$

where, $k_1 = \beta_1 I_a + \beta_2 I_h + \alpha_h + \mu_h$, $k_2 = \eta + \mu_h$, $k_3 = \beta_2 I_h + \beta_1 I_a$, $k_4 = \alpha_1 + \mu_h$, $k_5 = \alpha_2 + \delta_h + \mu_h$, $k_6 = \beta_3 I_a + \mu_a$, $k_7 = \beta_3 I_a$, and $Z = (\Lambda_h, 0,0,0,0, \Lambda_a, 0)^T$.

In the matrix K(Y), all off-diagonal entries are non-negative. Thus, it is the Metzler matrix. The vector Z is positive. This indicates that system (2.1) is positively invariant in $\mathbb{R}_7^+$, which means that any trajectory of (2.1) starting from an initial state remains in $\mathbb{R}_7^+$ forever.

3.2. Mpox-free equilibrium

The Mpox-free equilibrium (MFE) of system (2.1) is attained by equating each component of model system (2.1) to zero. Moreover, there are no illnesses or recoveries at the MFE. Consequently, the MFE of the Mpox model (2.1) is presented by

$$E_0 = \left(S_h^0, V_h^0, E_h^0, I_h^0, R_h^0, S_a^0, I_a^0\right) = \left(\frac{\Lambda_h}{\mu_h + \alpha_h}, 0,0,0,0, \frac{\Lambda_a}{\mu_a}, 0\right).$$

3.3. Reproduction number

In mathematical epidemiology, the basic reproduction number is a critical threshold. It assists in predicting the likelihood of disease transmission. To ascertain R_0, system (2.1) utilizes the next-generation matrix, giving

$$F = \begin{pmatrix} 0 & 0 & 0 & 0 \\ 0 & 0 & \beta_2 S_h & \beta_1 S_h \\ 0 & 0 & 0 & 0 \\ 0 & 0 & 0 & \beta_3 S_a \end{pmatrix}, \quad V = \begin{pmatrix} \eta + \mu_h & 0 & 0 & 0 \\ 0 & \alpha_1 + \mu_h & 0 & 0 \\ 0 & -\alpha_1 & \alpha_2 + \delta_h + \mu_h & 0 \\ 0 & 0 & 0 & \mu_a \end{pmatrix}.$$

The Monkeypox model's basic reproduction number is

$$\begin{aligned} R_0 &= \max\left\{\frac{\beta_3 S_a^0}{\mu_a}, \frac{\alpha_1 \beta_2 S_h^0}{(\alpha_1 + \mu_h)(\alpha_2 + \delta_h + \mu_h)}\right\} \\ &= \max\{\Re_a, \Re_h\}. \end{aligned}$$

3.4. Endemic equilibrium

The endemic equilibrium for the Mpox dynamical system (2.1) is

$$E_1 = (S_h^*, V_h^*, E_h^*, I_h^*, R_h^*, S_a^*, I_a^*),$$

where

$$S_h^* = \frac{\Lambda_h + \eta V_h^*}{(\beta_2 I_a^* + \beta_1 I_h^*) + \alpha_h + \mu_h}, \; V_h^* = \frac{\alpha_h S_h^*}{\eta + \mu_h},$$

$$E_h^* = \frac{(\beta_2 I_a^* + \beta_1 I_h^*) S_h^*}{\alpha_1 + \mu_h},\ I_h^* = \frac{\alpha_1 E_h^*}{\alpha_2 + \delta_h + \mu_h},$$

$$R_h^* = \frac{I_{h1}^* \alpha_2}{\mu_h}, S_a^* = \frac{\mu_a}{\beta_3}, I_a^* = \frac{\Lambda_a}{2\mu_a}.$$

4. Stability analysis of the Mpox model

4.1. Local stability of E_0

Theorem 4.1.1. System (2.1)'s MFE (E_0) is locally asymptotically stable if $R_0 < 1$, and unstable if $R_0 > 1$.

Proof. The Jacobian matrix at the Mpox-free equilibrium (E_0) is

$$J(E_0) = \begin{pmatrix} -(\alpha_h + \mu_h) & \eta & 0 & -\beta_2 S_h^0 & 0 & 0 & -\beta_1 S_h^0 \\ \alpha_h & -(\eta + \mu_h) & 0 & 0 & 0 & 0 & 0 \\ 0 & 0 & -(\alpha_1 + \mu_h) & \beta_2 S_h^0 & 0 & 0 & \beta_1 S_h^0 \\ 0 & 0 & \alpha_1 & -(\alpha_2 + \delta_h + \mu_h) & 0 & 0 & 0 \\ \alpha & 0 & 0 & \alpha_2 & -\mu_h & 0 & 0 \\ 0 & 0 & 0 & 0 & 0 & -\mu_a & -\beta_3 S_a^0 \\ 0 & 0 & 0 & 0 & 0 & 0 & \beta_3 S_a^0 - \mu_a \end{pmatrix}.$$

The eigenvalues for the matrix $J(E_0)$ are $-\mu_h$,$-\mu_a$, $-(\eta + \mu_h)$, $-(\alpha_h + \mu_h)$, $-(\alpha_1 + \mu_h)$, $\beta_2 S_h^0 - (\alpha_2 + \delta_h + \mu_h)$, and $\beta_3 S_a^0 - \mu_a$. Clearly, the first five eigenvalues are negative. Therefore, the MFE E_0 is locally asymptotically stable if

$$\beta_2 S_h^0 - (\alpha_2 + \delta_h + \mu_h) < 0,$$

$$\beta_2 S_h^0 < (\alpha_2 + \delta_h + \mu_h),$$

$$\frac{\beta_2 S_h^0}{(\alpha_2 + \delta_h + \mu_h))} < 1,$$

$$R_0 < 1,$$

and

$$\beta_3 S_a^0 - \mu_a < 0,$$

$$\mu_a \left(\frac{\beta_3 S_a^0}{\mu_a} - 1\right) < 0,$$

$$\mu_a (R_0 - 1) < 0,$$

$$R_0 < 1.$$

Hence, the MFE E_0 is locally asymptotically stable if $R_0 < 1$, otherwise it is unstable.

4.2. Global stability of Mpox-free equilibrium (E_0) & Endemic equilibrium (E_1)

Lemma 4.2.1. The region $\varpi_1 = \{X \epsilon \varpi_1 : S_h \leq S_h^0, S_a \leq S_a^0\}$ is positively invariant for model (2.1), where $X = \{S_h,\ V_h,\ E_h,\ I_h,\ R_h,\ S_a,\ I_a\}$.

Proof. Using the model's first equation, we obtain

$$\frac{dS_h}{dt} = \Lambda_h - \beta_1 S_h I_a - \beta_2 S_h I_h - \alpha_h S_h - \mu_h S_h + \eta V_h \leq \Lambda_h - \alpha_h S_h - \mu_h S_h$$

$$\leq (\alpha_h + \mu_h)\left(\frac{\Lambda_h}{(\alpha_h + \mu_h)} - S_h\right) \leq (\alpha_h + \mu_h)(S_h^0 - S_h).$$

This implies that $S_h \leq S_h^0 - \left(S_h^0 - S_h(0)\right)e^{-(\alpha_h+\mu_h)t}$. Thus, $S_h(t) \leq S_h^0$ for all $t \geq 0$.
Using the model's sixth equation, we obtain

$$\frac{dS_a}{dt} = \Lambda_a - \beta_3 S_a I_a - \mu_a S_a \leq \Lambda_2 - \mu_a S_a \leq \mu_a\left(\frac{\Lambda_a}{\mu_a} - S_a\right).$$

This implies that $S_a \leq S_a^0 - (S_a^0 - S_a(0))e^{-\mu_a t}$. Thus, $S_a(t) \leq S_a^0$ for all $t \geq 0$.
In summary, we conclude that ϖ_1 is positively invariant.
Theorem 4.2.1. The Mpox model may be expressed generally as

$$\frac{d\varkappa_1}{dt} = \mathcal{F}(\varkappa_1, \varkappa_2), \frac{d\varkappa_2}{dt} = G(\varkappa_1, \varkappa_2), G(\varkappa_1, 0) = 0, \tag{4.1}$$

where $\varkappa_1 = (S_h, V_h, R_h, S_a)^T$ and $\varkappa_2 = (E_h, I_h, I_a)^T$ represent the individuals who are infected and those who are not. Then, the MFE is now represented by the following:

$$E_0 = (\varkappa_1^0, 0) = \left(\frac{\Lambda_h}{(\alpha_h+\mu_h)}, \frac{\alpha_h\Lambda_h}{(\eta+\mu_h)(\alpha_h+\mu_h)}, 0, \frac{\Lambda_a}{\mu_a}, 0,0,0\right).$$

The following conditions must be met for E_0 to maintain global asymptomatic stability:
H_1: $\frac{d\varkappa_1}{dt} = \mathcal{F}(\varkappa_1^0, 0), \varkappa_1^0$ is globally asymptomatic stable,
H_2: $\widehat{G}(\varkappa_1, \varkappa_2) = A\varkappa_2 - G(\varkappa_1, \varkappa_2), \widehat{G}(\varkappa_1, \varkappa_2) \geq 0$, where $A = D_{\varkappa_2}\mathcal{F}(\varkappa_1^0, 0)$ is the Metzler matrix.
Theorem 4.2.2. If the criteria of equation (4.1) are met and $R_0 < 1$, then $E_0 = (\varkappa_1^0, 0)$ is a globally asymptomatically stable.
Proof. Applying theorem (4.2.1),

$$\mathcal{F}(\varkappa_1^0, 0) = \Lambda_h - \alpha_h S_h - \mu_h S_h, \hat{G}(\varkappa_1, \varkappa_2) = A\varkappa_2 - G(\varkappa_1, \varkappa_2),$$

where

$$A = \begin{bmatrix} -(\alpha_h + \mu_h) & \beta_2 S_h^0 & \beta_1 S_h^0 \\ \alpha_h & -(\alpha_2 + \delta_h + \mu_h) & 0 \\ 0 & 0 & \beta_3 S_a^0 - \mu_a \end{bmatrix}.$$

Now, $\widehat{G}(\varkappa_1, \varkappa_2) = A\varkappa_2 - G(\varkappa_1, \varkappa_2) = \begin{bmatrix} \beta_1 I_a(S_h^0 - S_h) + \beta_2 I_h(S_h^0 - S_h) \\ 0 \\ \beta_3 I_a(S_a^0 - S_a) \end{bmatrix} = \begin{bmatrix} \widehat{G}_1 \\ 0 \\ \widehat{G}_2 \end{bmatrix}$.
Clearly, $\widehat{G}_1 \geq 0$, and $\widehat{G}_2 \geq 0$, since $S_h \leq S_h^0, S_a \leq S_a^0$. Therefore, $\widehat{G}(\varkappa_1, \varkappa_2) \geq 0$.
Also, A is the Metzler matrix. Hence, the Mpox-free equilibrium E_0 is globally asymptotically stable.
Theorem 4.2.3. System (2.1)'s E_1 is globally asymptotically stable if $R_0 > 1$.
Proof. Constructing a Lyapunov function is a common method to prove global stability. Construct the following Lyapunov function:

$$L(t) = \frac{1}{2}[(S_h - S_h^*) + (V_h - V_h^*) + (E_h - E_h^*) + (I_h - I_h^*) + (R_h - R_h^*)]^2$$

$$+\frac{1}{2}[(S_a - S_a^*) + (I_a - I_a^*)]^2. \tag{4.2}$$

Taking the derivative of Eq (4.2), we can obtain

$$L'(t) = [(S_h - S_h^*) + (V_h - V_h^*) + (E_h - E_h^*) + (I_h - I_h^*) + (R_h - R_h^*)]\frac{d(S_h + V_h + E_h + I_h + R_h)}{dt}$$

$$+[(S_a - S_a^*) + (I_a - I_a^*)]\frac{d(S_a+I_a)}{dt} = (N_h - N_h^*)\frac{dN_h}{dt} + (N_a - N_a^*)\frac{dN_a}{dt}, \quad (4.3)$$

where

$$\frac{dN_h}{dt} = \Lambda_h - \mu_h N_h, \frac{dN_a}{dt} = \Lambda_a - \mu_a N_a,$$

$$N_h^* = S_h^* + V_h^* + E_h^* + I_h^* + R_h^* = \frac{\Lambda_h}{\mu_h+\alpha_h},$$

$$N_a^* = S_a^* + I_a^* = \frac{\Lambda_a}{\mu_a}. \quad (4.4)$$

Substituting (4.4) into (4.3), we can obtain

$$L'(t) = \left(N_h - \frac{\Lambda_h}{\mu_h + \alpha_h}\right)(\Lambda_h - \mu_h N_h) + \left(N_a - \frac{\Lambda_a}{\mu_a}\right)(\Lambda_a - \mu_a N_a)$$

$$\leq \left(N_h - \frac{\Lambda_h}{\mu_h + \alpha_h}\right)(\Lambda_h - \mu_h N_h) + \left(N_a - \frac{\Lambda_a}{\mu_a}\right)(\Lambda_a - \mu_a N_a)$$

$$= -\frac{1}{\mu_h + \alpha_h}(\Lambda_h - \mu_h N_h)^2 - \frac{1}{\mu_a}(\Lambda_a - \mu_a N_a)^2.$$

It is obvious that $L'(t) \leq 0$ and $L'(t) = 0 \Leftrightarrow S_h = S_h^*$, $V_h = V_h^*, E_h = E_h^*$, $I_h = I_h^*, R_h = R_h^*$, $S_a = S_a^*, I_a = I_a^*$. According to Lasalle's invariant set principle, the endemic equilibrium E_1 of system (2.1) at this time is globally asymptotically stable.

5. Mpox model's sensitivity analysis

The sensitivity measures of R_0 demonstrate the degree to which the basic reproduction number responds to variations in each model parameter [39]. Analyzing sensitivity reveals the parameters that exert the most significant impact on disease transmission, thereby assisting in the prioritization of control strategies. The normalized forward sensitivity index of R_0 relates to system (2.1)' parameter ϑ, which is signified by

$$\xi_{R_0}^{\vartheta} = \frac{\partial R_0}{\partial \vartheta} \cdot \frac{\vartheta}{R_0}. \quad (5.1)$$

The data presented in Table 2 and Figure 3 reveal that the sensitivity indices of R_0 show positive sensitivity values (e.g., $\Lambda_h, \beta_2, \alpha_1$), indicating that an increase in these parameters will lead to an increase in R_0. Conversely, negative values (e.g., $\mu_h, \alpha_h, \alpha_2, \delta_h$) suggest that increasing these parameters will result in a decrease in R_0. This increases the R_0 levels, hence augmenting the opportunity of spreading the disease. The human recruitment rate Λ_h (index = +1) indicates that a growing human population results in a greater number of susceptible individuals, thereby facilitating increased transmission. β_2 (Human-to-human transfer rate, index = +1) indicates that the factor substantially affects the dissemination of monkeypox. The transmission dynamics are significantly affected by intimate encounters inside households or public environments. Enhanced negative sensitivity parameters reduce R_0. The recovery rate of infected persons, indexed at –0.33, expedites

the reduction of infectious time, hence decreasing the probability of transmission. The vaccination rate index of –0.06 decreases the vulnerable population, thereby lowering R_0.

Table 2. Sensitivity measures of R_0.

Parameter	Sensitivity index
Λ_h	1
β_2	1
α_1	0.88235294
μ_h	-2.41273832
α_h	-0.0625
α_2	-0.32806324
δ_h	-0.07905138

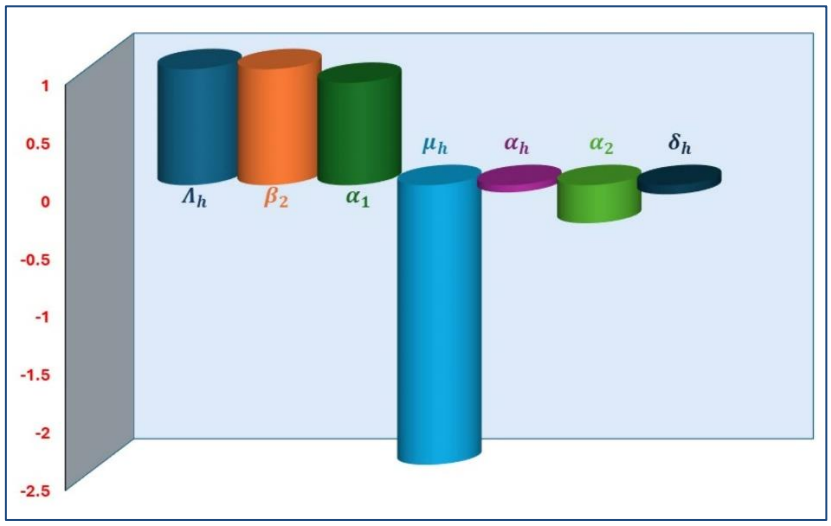

Figure 3. Sensitivity measures of R_0.

Figure 4 underscores the significance of enhancing recovery rates (α_2) and regulating the exposure-to-infection process (α_1) in mitigating the dissemination of monkeypox. A higher α_1 indicates that exposed individuals progress to an infectious state more swiftly, hence elevating the total transmission rate of the disease. A decreased α_1 impedes this transition, diminishing R_0 and decelerating the dissemination of the disease. An elevated α_2 indicates that infected individuals recuperate more swiftly, hence diminishing their duration in an infectious condition, which subsequently lowers R_0. A reduced α_2 prolongs the duration of infectiousness in individuals, hence elevating R_0.

Figure 5 underscores the pivotal function of vaccination (α_h) in diminishing R_0, while simultaneously indicating that lowering mortality (δ_h) is essential for human and successful disease management. A higher α_h indicates a greater percentage of the population is vaccinated, hence diminishing the number of vulnerable individuals and consequently lowering R_0. A reduced α_h signifies a diminished vaccination rate, leading to an expanded population of vulnerable individuals, hence elevating R_0 and the likelihood of outbreaks. A higher δ_h indicates an increased mortality rate among infected individuals, hence eliminating them from the transmission chain. Although this decreases R_0, it constitutes a detrimental health result and should not be employed as a technique for

disease control. A reduced δ_h indicates that a greater number of sick persons survive and remain infectious, perhaps resulting in an escalation of R_0 and ongoing disease transmission.

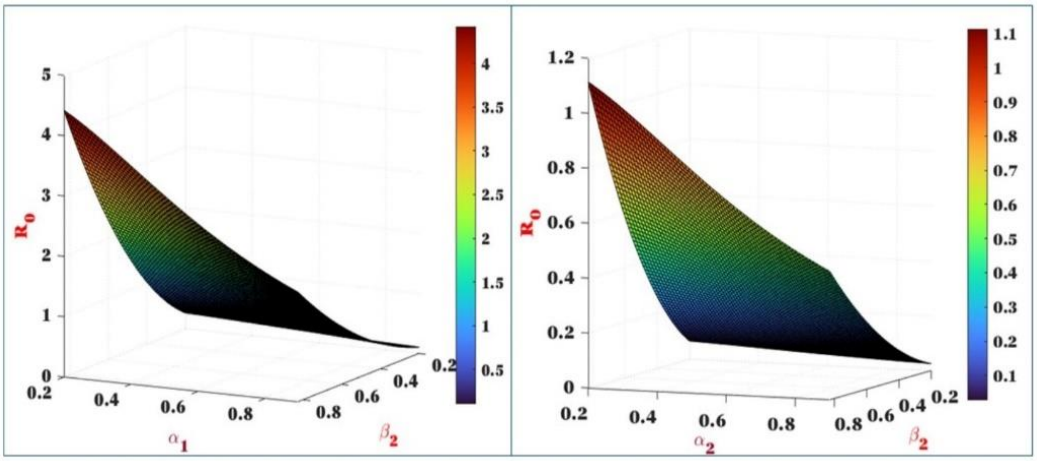

Figure 4. Impact of variability α_1 & α_2 on R_0.

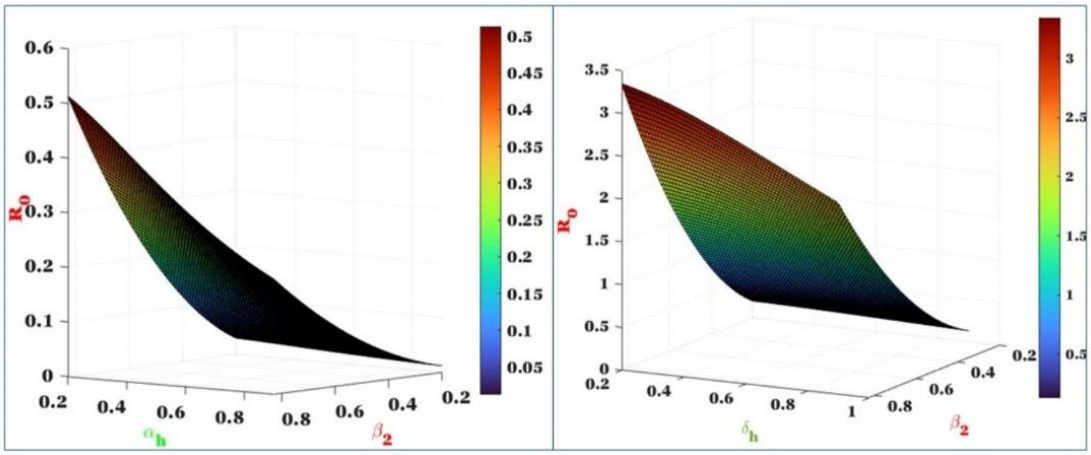

Figure 5. Impact of variability α_h & δ_h on R_0.

Figure 6 presents a contour graphic that analyzes the cumulative impacts of α_1 (the rate of progression from exposed to infected individuals), α_2 (the recovery rate of infected individuals), and β_2 (the human-to-human transmission rate) on R_0. The synergistic impact of α_1, α_2, and β_2 underscores that, although expedited recovery and diminished progression from exposed to infected individuals can lower R_0, mitigating transmission through interventions aimed at β_2 is the most efficient long-term approach for disease management.

Figure 7 presents a contour map demonstrating the impact of the interaction between α_h (vaccination rate in humans) and δ_h (disease-induced mortality) to β_2 (human-to-human transmission rate) on R_0. The contour figure indicates that elevated values of β_2 (increased transmission) result in a greater R_0, unless there is a substantial rise in α_h (vaccination). Elevated vaccination rates (α_h) can mitigate the impact of high β_2, maintaining R_0 at reduced levels despite increased transmissibility of the disease.

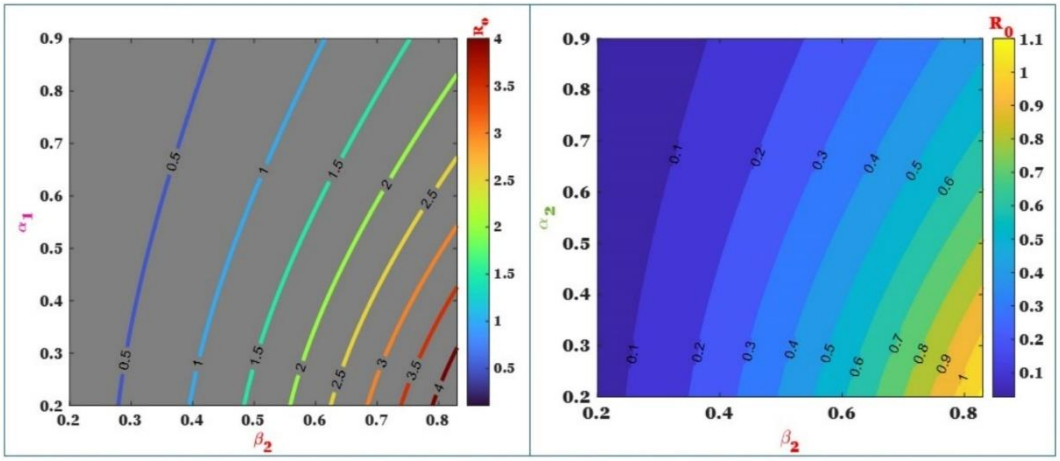

Figure 6. Contour plot of α_1 & α_2 on R_0.

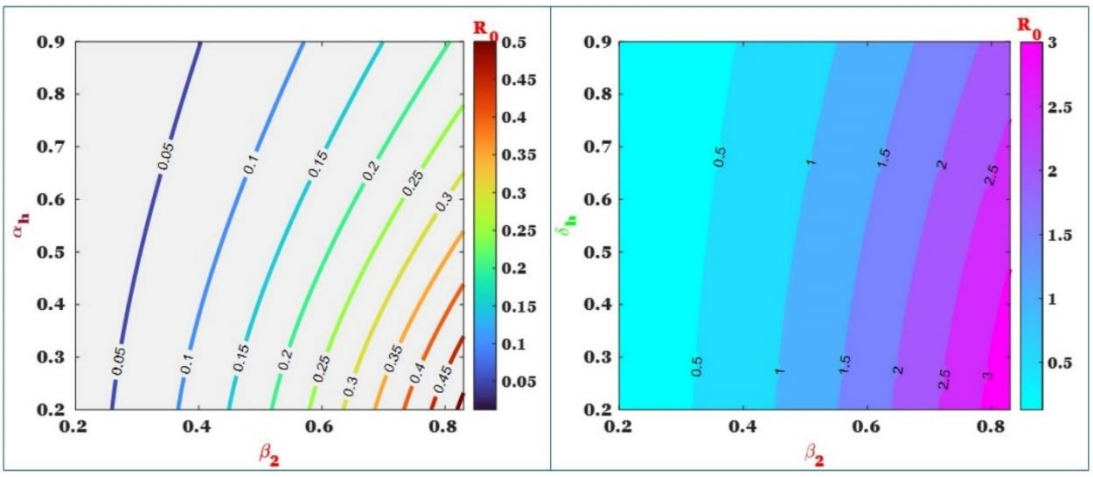

Figure 7. Contour plot of α_h & δ_h on R_0.

6. Numerical simulation

The model's numerical simulations are conducted using the parameter values indicated in Table 3 to illustrate the conclusions of the previous study. The simulation graphically illustrates the numbers of susceptible, vaccinated, exposed, and infected individuals in the host population, together with the number of susceptible rodents.

Table 3. References and parameter values of system (2.1).

Parameter	Values	Reference
Λ_h	1.925000	[40]
β_1	0.025000	[41]
α_h	0.010000	Assumed
β_2	0.063000	[42]
μ_h	0.005000	[43]
η	0.030000	Assumed
α_1	0.028000	[44]
δ_h	0.020000	Assumed
α_2	0.083000	[45]
Λ_a	0.112000	[46]
β_3	0.027000	[47]
μ_a	0.000016	[48]

Figure 8 has four panels depicting the impact of β_1 (transmission rate from infected rodent to humans) on the dynamics of vaccinated humans (V_h), infected humans (I_h), exposed people (E_h), and the overall human population ($V_h + I_h + E_h$) over time. As β_1 escalates, the quantity of vaccinated individuals rises more swiftly owing to the heightened risk for disease. With an elevated β_1 (red curve), the incidence of infected individuals escalates more rapidly, signifying accelerated disease transmission. A reduced β_1 (blue curve) results in a more gradual rise in infections. The quantity of exposed humans fluctuates in accordance with variations in the rodent-to-human transmission rate, with elevated β_1 resulting in a greater number of exposed persons. The total human population curve illustrates the collective dynamics of vaccinated, exposed, and infected individuals, indicating that elevated transmission rates augment the overall number of individuals impacted by the disease.

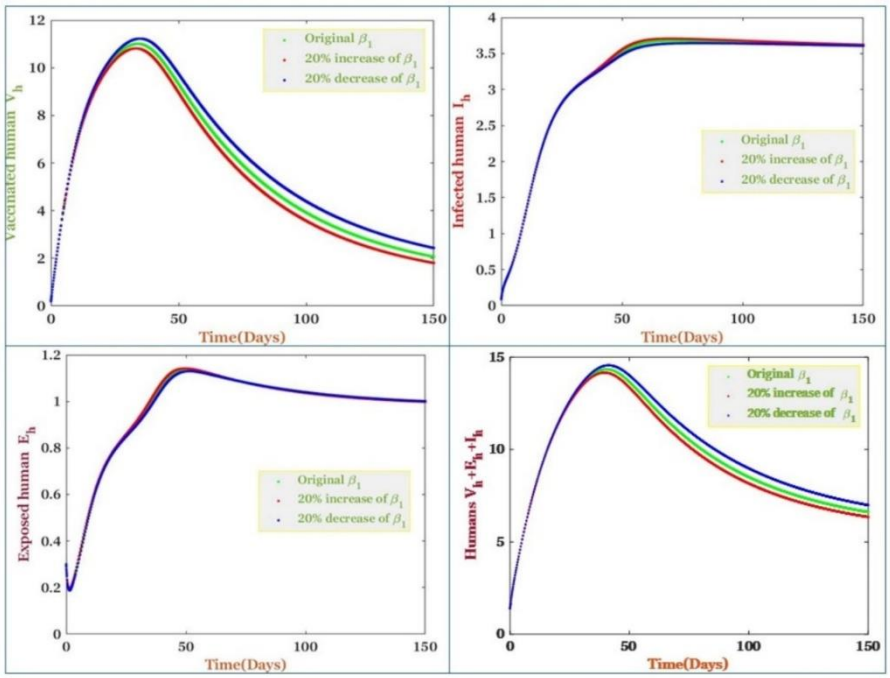

Figure 8. The effects of β_1 on diverse population.

Figure 9 comprises four panels that depict the impact of variations in β_2 (the human-to-human transmission rate) on the dynamics of vaccinated humans (V_h), infected humans (I_h), exposed people (E_h), and the overall human population ($V_h + I_h + E_h$) over time. Top-left: As β_2 grows, vaccination rates (V_h) first escalate more rapidly due to the heightened infection risk. Nonetheless, a reduction in β_2 results in a deceleration in vaccination rates. Top-right: A 20% augmentation in β_2 results in an accelerated dissemination of the disease, evidenced by a more rapid growth in the infected population. A 20% reduction in β_2 indicates a decline in the number of exposed individuals over time due to diminished disease transmission efficacy. The figure underscores the significance of transmission rates (β_2) in influencing disease patterns. Elevated transmission rates result in expedited vaccination responses and accelerated disease dissemination, whereas diminished transmission rates decelerate the entire process.

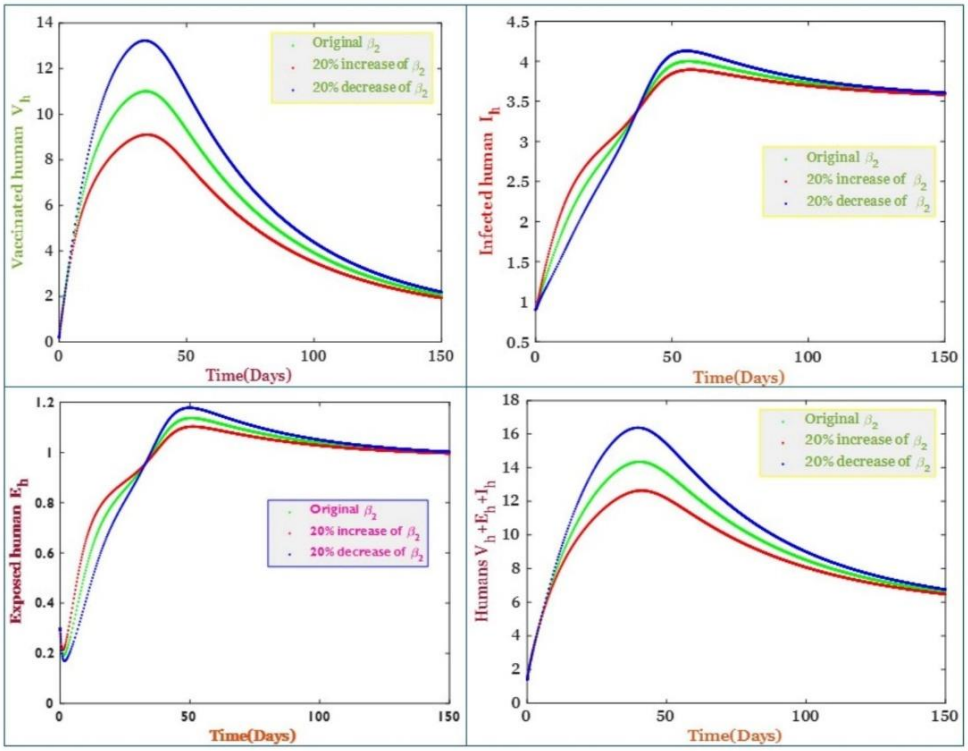

Figure 9. The effects of β_2 on diverse population.

The Figure 10 comprises four panels depicting the temporal dynamics of susceptible humans (S_h), vaccinated humans (V_h), susceptible rodents (S_a), and the aggregate human and rodent population ($S_h + V_h + S_a$), while analyzing the impact of varying levels of β_3 (infection rate from infected rodent to susceptible rodent). This picture illustrates how the transmission rate between rodents substantially influences disease dynamics and the population's reaction to vaccination. A greater β_3 (red curve) results in a more rapid decline of susceptible populations (both human and rodent), an accelerated increase in vaccinated humans, and a decelerated overall population growth attributable to elevated infection rates. A reduced β_3 (blue curve) leads to decelerated disease transmission, resulting in a slower decline of susceptible populations, alongside a more gradual rise in vaccinations and population growth.

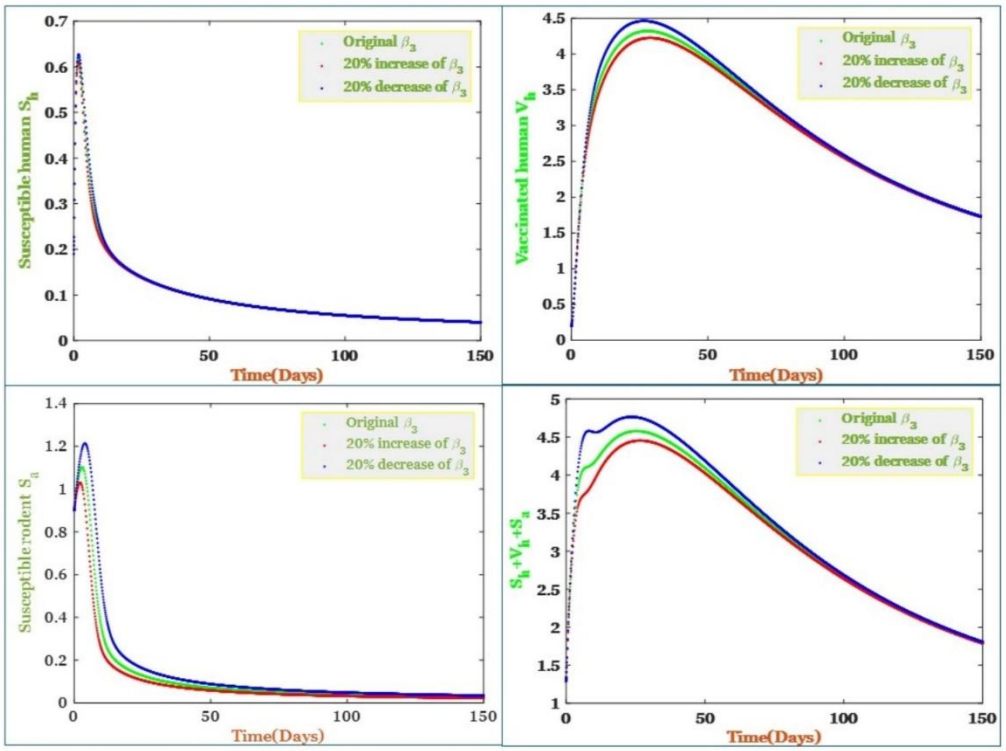

Figure 10. Effects of β_3 on diverse population.

It is important to note that many existing Monkeypox models rely primarily on local stability analysis, typically using linearization techniques around equilibrium points. While such methods provide valuable insights near equilibria, they do not account for the full system behavior under broader perturbations. In contrast, our use of a Lyapunov-based global stability framework ensures that the system trajectories converge to equilibrium from any biologically feasible initial condition. This global perspective is particularly relevant in epidemiological settings, where initial infection levels, transmission dynamics, or vaccination rates may vary significantly across populations. By offering stronger predictive power and robustness, our approach provides a more reliable basis for long-term public health planning and disease control strategies.

7. Conclusions

This paper introduces a detailed mathematical model that encapsulates the transmission dynamics of the Monkeypox virus (Mpox) by incorporating human-to-human, rodent-to-human, and rodent-to-rodent transmission routes. The key innovation lies in the integration of dual-species transmission dynamics with vaccination waning effects, providing a more comprehensive and biologically realistic representation of Mpox spread. The model integrates essential epidemiological parameters, including exposure progression, recovery, and disease-induced mortality, and ensures mathematical rigor through the analysis of positivity, boundedness, and global asymptotic stability using Lyapunov functions. Sensitivity analysis highlights the most influential parameters affecting the basic reproduction number, offering valuable insight into targeted intervention strategies. Numerical simulations confirm the analytical findings and illustrate the significant effects of key parameters such as vaccination coverage, recovery rate, and rodent-related transmission rates on outbreak severity and trajectory. However, the present study is limited by the use of assumed or literature-based parameter

values in the absence of real-time epidemiological datasets. This constraint may affect the precision of specific quantitative predictions, particularly for region-specific outbreak scenarios. Future research should incorporate data-driven parameter estimation using recent and localized Mpox case reports, enabling more accurate and validated model outputs. Additionally, the framework can be extended to include spatial heterogeneity (e.g., urban-rural mobility or environmental reservoirs) and behavioral compartments that reflect changes in human behavior, such as risk aversion or vaccine hesitancy, during outbreaks. These enhancements will further increase the model's applicability for dynamic public health response planning.

Author contributions

Turki D. Alharbi: Methodology, writing, review and editing; Md Rifat Hasan: Conceptualization, methodology, software, formal analysis, writing, review and editing. All authors have read and agreed to the published version of the manuscript.

Use of Generative-AI tools declaration

The authors declare they have not used Artificial Intelligence (AI) tools in the creation of this article.

Conflict of interest

The authors declare that the research was conducted in the absence of any conflict of interest.

References

1. B. Y. Liu, S. L. Jing, H. Xiang, H. F. Huo, Modeling the transmission dynamic of Mpox virus with Vertical transmission, *Math. Method. Appl. Sci.*, **48** (2025), 13517–13529. https://doi.org/10.1002/MMA.11119
2. F. A. Wireko, J. N. Martey, I. K. Adu, B. E. Owusu, S. Ndogum, J. K. K. Asamoah, Modeling the impact of double-dose vaccination and saturated transmission dynamics on Mpox control, *Eng. Rep.*, **7** (2025), 1–24. https://doi.org/10.1002/ENG2.70144
3. M. Helikumi, F. Ojija, A. Mhlanga, Dynamical analysis of Mpox disease with environmental effects, *Fractal Fract.*, **9** (2025), 1–27. https://doi.org/10.3390/FRACTALFRACT9060356
4. O. J. Peter, C. E. Madubueze, M. M. Ojo, F. A. Oguntolu, T. A. Ayoola, Modeling and optimal control of monkeypox with cost-effective strategies, *Model. Earth Syst. Env.*, **9** (2023), 1989–2007. https://doi.org/10.1007/S40808-022-01607-Z
5. H. Harapan, Y. Ophinni, D. Megawati, A. Frediansyah, S. S. Mamada, M. Salampe, et al., Monkeypox: A comprehensive review, *Viruses*, **14** (2022), 1–24. https://doi.org/10.3390/V14102155
6. M. B. Martinez, Y. Yang, B. Jafari, A. Kaur, Z. A. Butt, H. H. Chen, et al., Monkeypox: A review of epidemiological modelling studies and how modelling has led to mechanistic insight, *Epidemiol. Infect.*, **151** (2023), 1–16. https://doi.org/10.1017/S0950268823000791
7. A. Venkatesh, M. Manivel, K. Arunkumar, M. P. Raj, Shyamsunder, S. D. Purohit, A fractional mathematical model for vaccinated humans with the impairment of Monkeypox transmission, *Eur. Phys. J.-Spec. Top.*, **2024** (2024), 1–21. https://doi.org/10.1140/EPJS/S11734-024-01211-5

8. W. Okongo, J. O. Abonyo, D. Kioi, S. E. Moore, S. N. Aguegboh, Mathematical modeling and optimal control analysis of Monkeypox virus in contaminated environment, *Model. Earth Syst. Env.*, **10** (2024), 3969–3994. https://doi.org/10.1007/S40808-024-01987-4
9. S. Okyere, J. A. Prah, Modeling and analysis of Monkeypox disease using fractional derivatives, *Results Eng.*, **17** (2023), 100786–100794. https://doi.org/10.1016/j.rineng.2022.100786
10. J. Molla, I. Sekkak, A. M. Ortiz, I. Moyles, B. Nasri, Mathematical modeling of Mpox: A scoping review, *One Health*, **16** (2023), 100540–100547. https://doi.org/10.1016/J.ONEHLT.2023.100540
11. W. Adel, A. Elsonbaty, A. Aldurayhim, A. E. Mesady, Investigating the dynamics of a novel fractional-order monkeypox epidemic model with optimal control, *Alex. Eng. J.*, **73** (2023), 519–542. https://doi.org/10.1016/J.AEJ.2023.04.051
12. A. Omame, A. A. Raezah, G. A. Okeke, T. Akram, A. Iqbal, Assessing the impact of intervention measures in a mathematical model for monkeypox and COVID-19 co-dynamics in a high-risk population, *Model. Earth Syst. Env.*, **10** (2024), 6341–6355. https://doi.org/10.1007/S40808-024-02132-X
13. M. R. Hasan, A. Hobiny, A. Alshehri, Analysis of Vector-host SEIR-SEI Dengue epidemiological model, *Int. J. Anal. Appl.*, **20** (2022), 1–19. https://doi.org/10.28924/2291-8639-20-2022-57
14. W. Okongo, J. A. Okelo, D. K. Gathungu, S. E. Moore, S. A. Nnaemeka, Transmission dynamics of Monkeypox virus with age-structured human population: A mathematical modeling approach, *J Appl. Math.*, **2024** (2024), 1–17. https://doi.org/10.1155/2024/9173910
15. T. D. Alharbi, M. R. Hasan, Global stability and sensitivity analysis of vector-host dengue mathematical model, *AIMS Math.*, **9** (2024), 32797–32818. https://doi.org/10.3934/MATH.20241569
16. O. J. Peter, A. Abidemi, M. M. Ojo, T. A. Ayoola, Mathematical model and analysis of Monkeypox with control strategies, *Eur. Phys. J. Plus*, **138** (2023), 1–20. https://doi.org/10.1140/EPJP/S13360-023-03865-X
17. P. Kumar, M. Vellappandi, Z. A. Khan, S. M. Sivalingam, A. Kaziboni, V. Govindaraj, A case study of Monkeypox disease in the United States using mathematical modeling with real data, *Math. Comput. Simulat.*, **213** (2023), 444–465. https://doi.org/10.1016/J.MATCOM.2023.06.016
18. F. M. Allehiany, M. H. DarAssi, I. Ahmad, M.A. Khan, E. M. Tag-Eldin, Mathematical modeling and backward bifurcation in Monkeypox disease under real observed data, *Results Phys*., **50** (2023), 106557–106570. https://doi.org/10.1016/J.RINP.2023.106557.
19. K. Soni, A. K. Sinha, Modeling and stability analysis of the transmission dynamics of Monkeypox with control intervention, *Part. Differ. Equ. Appl. Math.*, **10** (2024), 100730–100746. https://doi.org/10.1016/J.PADIFF.2024.100730
20. T. D. Awoke, S. M. Kassa, Y. A. Terefe, M. D. Asfaw, Modeling on cost-effectiveness of monkeypox disease control strategies with consideration of environmental transmission effects in the presence of vaccination, *Model. Earth Syst. Env.*, **10** (2024), 6105–6132. https://doi.org/10.1007/S40808-024-02108-X
21. A. Alshehri, S. Ullah, Optimal control analysis of Monkeypox disease with the impact of environmental transmission, *AIMS Math.*, **8** (2023), 16926–16960 https://doi.org/10.3934/MATH.2023865
22. D. Bentaleb, Z. Khatar, S. Amine, Epidemiological modeling of Monkeypox clades: A dual-strain SEIR approach with stability, bifurcation, and sensitivity analysis, *Model. Earth Syst. Env.*, **10** (2024), 6949–6963. https://doi.org/10.1007/S40808-024-02162-5
23. Y. Guo, T. Li, Modeling the competitive transmission of the Omicron strain and Delta strain of COVID-19, *J. Math. Anal. Appl.*, **526** (2023). https://doi.org/10.1016/j.jmaa.2023.127283

24. T. Li, Y. Guo, Modeling and optimal control of mutated COVID-19 (Delta strain) with imperfect vaccination, *Chaos Soliton. Fract.*, **156** (2022), 111825–111844. https://doi.org/10.1016/J.CHAOS.2022.111825
25. Y. Guo, T. Li, Fractional-order modeling and optimal control of a new online game addiction model based on real data, *Commun. Nonlinear Sci.*, **121** (2023), 107221. https://doi.org/10.1016/J.CNSNS.2023.107221
.26. M. Manivel, A. Venkatesh, S. Kumawat, Numerical simulation for the co-infection of Monkeypox and HIV model using fractal-fractional operator, *Model. Earth Syst. Env.*, **11** (2025), 1–24. https://doi.org/10.1007/S40808-025-02359-2
27. A. Omame, S. A. Iyaniwura, Q. Han, A. Ebenezer, N. L. Bragazzi, X. Wang, et al., Dynamics of Mpox in an HIV endemic community: A mathematical modelling approach, *Math. Biosci. Eng.*, **22** (2025), 225–259. https://doi.org/10.3934/MBE.2025010
28. N. L. Bragazzi, Q. Han, S. A. Iyaniwura, A. Omame, A. Shausan, X. Wang, et al., Adaptive changes in sexual behavior in the high-risk population in response to human Monkeypox transmission in Canada can help control the outbreak: Insights from a two-group, two-route epidemic model, *J Med. Virol.*, **95** (2023), 1–12. https://doi.org/10.1002/JMV.28575
29. B. Liu, S. Farid, S. Ullah, M. Altanji, R. Nawaz, S. W. Teklu, Mathematical assessment of monkeypox disease with the impact of vaccination using a fractional epidemiological modeling approach, *Sci. Rep.*, **13** (2023), 1–27. https://doi.org/10.1038/S41598-023-40745-X
30. J. Bansal, A. Kumar, A. Kumar, A. Khan, T. Abdeljawad, Investigation of monkeypox disease transmission with vaccination effects using fractional order mathematical model under Atangana-Baleanu Caputo derivative, *Model. Earth Syst. Env.*, **11** (2025), 1–25. https://doi.org/10.1007/S40808-024-02202-0
31. J. Kongson, C. Thaiprayoon, W. Sudsutad, Analysis of a mathematical model for the spreading of the monkeypox virus with constant proportional-Caputo derivative operator, *AIMS Math.*, **10** (2025), 4000–4039. https://doi.org/10.3934/MATH.2025187
32. S. Rashid, A. Bariq, I. Ali, S. Sultana, A. Siddiqa, S. K. Elagan, Dynamic analysis and optimal control of a hybrid fractional monkeypox disease model in terms of external factors, *Sci. Rep.*, **15** (2025), 2944. https://doi.org/10.1038/S41598-024-83691-Y
33. F. O. Ochieng, Mathematical modeling of Mpox virus dynamics with a case study of Africa, *Model. Earth Syst. Env.*, **11** (2025), 1–21. https://doi.org/10.1007/S40808-025-02369-0
34. Shyamsunder, M. Meena, A comparative analysis of vector-borne disease: Monkeypox transmission outbreak, *J Appl. Math. Comput.*, **71** (2025), 1–37. https://doi.org/10.1007/S12190-025-02468-2
35. I. O. Idisi, K. Oshinubi, V. B. Sewanu, M. M. Yahaya, O. S. Olagbami, H. O. Edogbanya, Investigating Mpox strain dynamics using computational and data-driven approaches, *Viruses*, **17** (2025), 154. https://doi.org/10.3390/V17020154
36. M. Rabiu, E. J. Dansu, O. A. Mogbojuri, I. O. Idisi, M. M. Yahaya, P. Chiwira, et al., Modeling the sexual transmission dynamics of Mpox in the United States of America, *Eur. Phys. J. Plus*, **139** (2024), 1–20. https://doi.org/10.1140/EPJP/S13360-024-05020-6
37. K. Kuga, J. Tanimoto, Which is more effective for suppressing an infectious disease: Imperfect vaccination or defense against contagion? *J. Stat. Mech.-Theory E.*, **2018** (2018), 023407. https://doi.org/10.1088/1742-5468/AAAC3C
38. J. Tanimoto, *Sociophysics approach to epidemics*, Singapore: Springer Singapore, 2021. https://doi.org/10.1007/978-981-33-6481-3

39. M. R. Hasan, A. Hobiny, A. Alshehri, Sensitivity analysis of Vector-host dynamic Dengue epidemic model, *Commun. Math. Appl.*, **14** (2023), 1001–1017. https://doi.org/10.26713/CMA.V14I2.2119
40. M. Qian, D. Li, Z. Hao, S. Hu, W. Li, An epidemiological model of Monkeypox: Model prediction and control application, *BMC Infect. Dis.*, **25** (2025), 1–16. https://doi.org/10.1186/S12879-025-10873-Y
41. M. A. I. Islam, M. H. M. Mubassir, A. K. Paul, S. S. Shanta, A mathematical model for understanding and controlling monkeypox transmission dynamics in the USA and its implications for future epidemic management, *Decod. Infect. Transm.*, **2** (2024), 100031. https://doi.org/10.1016/J.DCIT.2024.100031
42. E. Addai, M. Ngungu, M. A. Omoloye, E. Marinda, Modelling the impact of vaccination and environmental transmission on the dynamics of monkeypox virus under Caputo operator, *Math. Biosci. Eng.*, **20** (2023), 10174–10199. https://doi.org/10.3934/MBE.2023446
43. M. Al Qurashi, S. Rashid, A. M. Alshehri, F. Jarad, F. Safdar, New numerical dynamics of the fractional monkeypox virus model transmission pertaining to nonsingular kernels, *Math. Biosci. Eng.*, **20** (2023), 402–436. https://doi.org/10.3934/MBE.2023019
44. A. Khan, Y. Sabbar, A. Din, Stochastic modeling of the Monkeypox 2022 epidemic with cross-infection hypothesis in a highly disturbed environment, *Math. Biosci. Eng.*, **19** (2022), 13560–13581. https://doi.org/10.3934/MBE.2022633
45. S. Li, Samreen, S. Ullah, S. A. AlQahtani, S. M. Tag, A. Akgül, Mathematical assessment of Monkeypox with asymptomatic infection: Prediction and optimal control analysis with real data application, *Results Phys.*, **51** (2023), 106726. https://doi.org/10.1016/J.RINP.2023.106726
46. Samreen, S. Ullah, R. Nawaz, A. Alshehri, Mathematical modeling of monkeypox infection with optimized preventive control analysis: A case study with 2022 outbreak, *Eur. Phys. J. Plus*, **138** (2023), 1–34. https://doi.org/10.1140/EPJP/S13360-023-04305-6
47. S. Usman, I. I. Adamu, Modeling the transmission dynamics of the Monkeypox virus infection with treatment and vaccination interventions, *J. Appl. Math. Phys.*, **5** (2017), 2335–2353. https://doi.org/10.4236/JAMP.2017.512191
48. O. J. Peter, S. Kumar, N. Kumari, F. A. Oguntolu, K. Oshinubi, R. Musa, Transmission dynamics of Monkeypox virus: A mathematical modelling approach, *Model. Earth Syst. Env.*, **8** (2022), 3423–3434. https://doi.org/10.1007/S40808-021-01313-2